Pergamon

Geochimica et Cosmochimica Acta, Vol. 66, No. 17, pp. 3093–3107, 2002

0016-7037/02 $22.00 + .00

PII S0016-7037(02)00879-7

# Paleoenvironmental reconstruction from chemical and isotopic compositions of Permo-Pennsylvanian pedogenic minerals

NEIL JOHN TABOR,[1,*] ISABEL P. MONTANEZ[1] and RANDAL J. SOUTHARD[2]

[1]Department of Geology, University of California, One Shields Avenue, Davis, CA 95616, USA
[2]Department of Land, Air, and Water Resources, University of California, Davis, CA 95616, USA

(*Received July* 24, 2001; *accepted in revised form February* 22, 2002)

**Abstract**—Mineralogical and chemical analysis of Late Pennsylvanian and Early Permian paleosols from the eastern shelf of the Midland basin, north-central Texas, USA, are used to test hypothesized climate change in Late Paleozoic western equatorial Pangea, previously defined independently on the bases of sedimentologic and paleontologic proxies and climate models. The $<0.2$-$\mu$m size phyllosilicate fraction in the studied paleosols exhibits down-profile trends in mineralogy and chemical composition that are consistent with modern weathering profiles suggesting a dominantly pedogenic origin. A stratigraphic trend from kaolinite-dominated profiles in Upper Pennsylvanian paleosols to profiles dominated by smectite and hydroxy-interlayered 2:1 phyllosilicates in Lower Permian paleosols indicates a relatively rapid decrease in soil weathering and leaching in the latest Pennsylvanian followed by a more gradual decrease in leaching throughout the Early Permian. The chemical composition (cation ratios and exchange capacity) of these phyllosilicates further corroborates this shift toward less intensive leaching, presumably in response to climate change from humid to progressively more arid conditions.

The phyllosilicates in the $<0.2$-$\mu$m size fraction and contemporaneous pedogenic calcites from the Permo-Pennsylvanian paleosols exhibit a long-term stratigraphic increase in their $\delta^{18}O$ values of as much as $\sim$3.2‰ and $\sim$5.2‰, respectively. This long-term trend is consistent with a transition throughout the latest Pennsylvanian through Early Permian toward progressively more evaporatively enriched soil waters. Superimposed on the long-term trend is an apparent rapid enrichment (1.5 to 2‰) in phyllosilicate $\delta^{18}O$ values immediately above the Pennsylvanian–Permian boundary. Observed oxygen isotope fractionation between the phyllosilicates and calcites within individual paleosols indicate isotopic disequilibrium between mineral pairs. This is attributed to a minor detrital component in the pedogenic clay-dominated phyllosilicate fraction coupled with the effects of seasonality of mineral formation. Inferred $\delta^{18}O$ compositions of Late Paleozoic meteoric water ($-2$‰ to $+4$‰) are compatible with less intensive soil leaching under conditions of increasing aridity, possibly coupled with a shift in local precipitation from a continental source to a marine source. *Copyright © 2002 Elsevier Science Ltd*

## 1. INTRODUCTION

Soils are strongly influenced by the climate under which they form and can be useful proxies of weathering and climate conditions. The mineralogical and chemical composition of pedogenic phyllosilicates, which form in a soil through alteration of detrital clays or by primary precipitation, are strongly controlled by the chemical activity of the soil solution, which in turn is influenced by the amount and seasonality of rainfall (Sparks, 1995; Buol et al., 1997). Soil weathering often produces changes in clay mineralogy from weathered micas to smectites, kaolinites, and iron-oxyhydroxides, a trend reflected in a decrease in Si:Al ratios and cation exchange capacity (of residual minerals) with increasing duration and intensity of pedogenesis. The intensity of pedogenesis is related to climatic conditions affecting temperature and the amount and distribution of precipitation. Pedogenic phyllosilicates (kaolinite, smectite) (Lawrence and Taylor, 1971, 1972) and coexisting pedogenic carbonates (Stern et al., 1997) have been shown to precipitate in isotopic equilibrium with the soil water in which they form and thus to record the $\delta^{18}O$ composition of soil water. Studies have suggested that the $\delta^{18}O$ composition of these pedogenic minerals can be related to the $\delta^{18}O$ composition of local meteoric water (Cerling and Quade, 1993; Lui et al., 1995; Amundson et al., 1996; Elliot et al., 1997; Stern et al., 1997; Deutz et al., 2001). The soil water, however, may not be isotopically identical to local precipitation because of the effects of fluid–rock interaction, evaporation, and transpiration on soil water $\delta^{18}O$ values (Hsieh et al., 1998; Savin and Hsieh, 1998).

The mineralogic, chemical, and isotopic composition of pedogenic minerals from paleosols are thus potentially powerful proxies of paleoenvironmental and paleoclimatic conditions. In contrast to the application of pedogenic carbonates to paleoclimate reconstructions, the mineralogic and geochemical composition of pedogenic phyllosilicates as paleoclimate proxies has been relatively little studied (e.g., Bird and Chivas, 1988, 1989; Stern et al., 1997; Giral-Kacmarcik et al., 1999). This in part reflects that the fine phyllosilicate fraction in paleosols can be a mixture of pedogenic clays, detrital and burial authigenic clays, and diagenetically altered pedogenic clays. To infer paleoclimate conditions from pedogenic phyllosilicates, it is necessary to document that they have not undergone extensive diagenetic alteration. Further, it is necessary to either isolate a pure pedogenic and preferably monomineralic phyllosilicate fraction or to characterize the effect

* Author to whom correspondence should be addressed (tabor@geology.ucdavis.edu).

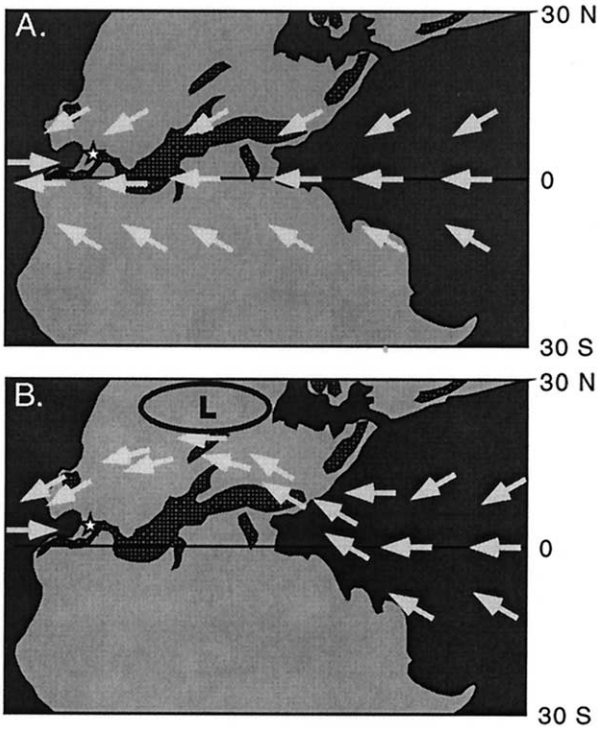


Fig. 1. Paleogeographic reconstruction of Late Pennsylvanian–Early Permian Pangea (30°N and S). Dark gray = ocean and inland seas; light gray = land; hatched pattern = major Late Paleozoic highlands; star = location of study area. Left-pointing arrows represent (A) zonal and (B) monsoonal atmospheric circulation proposed for this time period (Rowley et al., 1985; Parrish, 1993). Right-pointing arrows in (A) and (B) indicate superimposed regional-scale circulation over the Midland Basin hypothesized in this study.

of nonpedogenic clays on measured values and inferred soil conditions.

In this study, we present the mineralogic, chemical, and oxygen isotope compositions of paired pedogenic phyllosilicates and calcites from Upper Pennsylvanian through Early Permian paleosols of north-central Texas, USA, and use these values to test hypothesized models of climate conditions and atmospheric circulation over Late Paleozoic western equatorial Pangea (Fig. 1). We begin with a description of the mineralogy of the $<2$-$\mu$m size fraction of phyllosilicate minerals in paleosol profiles to delineate down-profile trends in pedogenic clay mineralogy. For comparison, we also present the down-profile trend in clay mineralogy ($<2$-$\mu$m size fraction) of a modern soil profile from the northern Sierra Nevada foothills of California, USA. Mineralogic trends in the $<2$-$\mu$m size phyllosilicate fraction in the Permo-Pennsylvanian paleosol profiles are consistent with modern soil weathering patterns, indicating that these phyllosilicates are dominated by pedogenic clays and therefore have paleoenvironmental and paleoclimatic significance. We subsequently present the chemical and $\delta^{18}O$ composition of the $<0.2$-$\mu$m size phyllosilicate fraction from B-horizons in the Permo-Pennsylvanian paleosols. Finally, we evaluate the utility of these chemical and isotopic properties as proxies for the composition of paleosoil water and paleoprecipitation and for interpreting changes in paleoatmospheric circulation over western equatorial Pangea during Late Paleozoic time.

The dominantly terrestrial Upper Pennsylvanian and Lower Permian succession of north-central Texas was deposited in three broad depositional belts (lower and upper coastal plain, and piedmont facies) distributed across the low-sloping eastern shelf of the Midland basin. The succession comprises ~800 m of upward fining fluvioalluvial cycles (Fig. 2; Hentz, 1988) and contains well-developed paleosols. The paleosols analyzed in this study are developed within lithic-dominated, clay-rich siltstones and claystones of overbank-floodplain deposits. The study area remained in the western equatorial region of Pangea, between the equator and 10° N throughout the Permo-Pennsylvanian (Scotese, 1984; Van der Voo et al., 1984).

Multiple fusilinid-bearing limestones (black units on Fig. 2) and regionally extensive fluvial sandstone sets (SS units on Fig. 2; Hentz, 1988) are intercalated throughout the succession and define a high-resolution stratigraphic framework for correlation throughout the study region. Two stratigraphic boundaries are well defined within the succession and provide the only absolute age control for this interval. The Pennsylvanian–Permian boundary (301 ± 2 Ma; Rasbury et al., 1998) occurs within the uppermost Markley Formation of the Bowie Group (Dunbar et al., 1960). The Wolfcampian–Leonardian boundary (283 ± 2 Ma; Ross et al., 1994) within the Lower Permian is defined by the fusilinid-bearing Elk City Limestone, which occurs in the lowermost Petrolia Formation of the Wichita Group (Fig. 2).

Paleosols are an important stratigraphic component of the Upper Pennsylvanian and Lower Permian succession of north-central Texas (Tabor and Montañez, unpublished data). Tabor and Montañez defined eight pedotypes (cf. Retallack, 1994) on the basis of macro- and micromorphologic characteristics of the paleosols. They interpreted the stratigraphic distribution of pedotypes to record a relatively rapid transition from humid conditions typical of the Late Pennsylvanian to significantly drier conditions in the earliest Permian. A climate trend toward increasingly drier conditions is recorded throughout the Lower Permian paleosols. Moreover, the paleosols proximal to the Pennsylvanian–Permian boundary record a rapid onset of sea-

Fig. 2. (A) Uppermost Pennsylvanian (Virgilian) and Lower Permian succession across a southwest-to-northeast trending section from the Eastern Shelf of the Midland Basin. White = mudrocks; light stipple = fluvial sandstone sets; dark gray = marine limestones; black = mappable coals. Modified from Hentz (1988). The black dots correspond to samples 1 to 12, from bottom to top, in Tables 1 and 2 and in Fig. 10. Open circles correspond to locations where only calcite $\delta^{18}O$ data are presented in Table 2 and Fig. 9 except for two sampling sites at 782 and 840 m in the Clear Fork Group, which are not shown. The northeastern end of the succession represents the northern extent of Permo-Pennsylvanian surficial outcrop in the study area (i.e., the Red River and Cretaceous overlap), whereas the southern end of the succession roughly corresponds to the 33°N latitude line in (B). (B) A regional geologic map of northern Texas, USA; inset map of Texas gives approximate location of study area. The black dots correspond to samples 1 to 12 in Tables 1 and 2 and Fig. 10. White dots correspond to locations where only calcite $\delta^{18}O$ data are presented in Table 2 and Fig. 9.

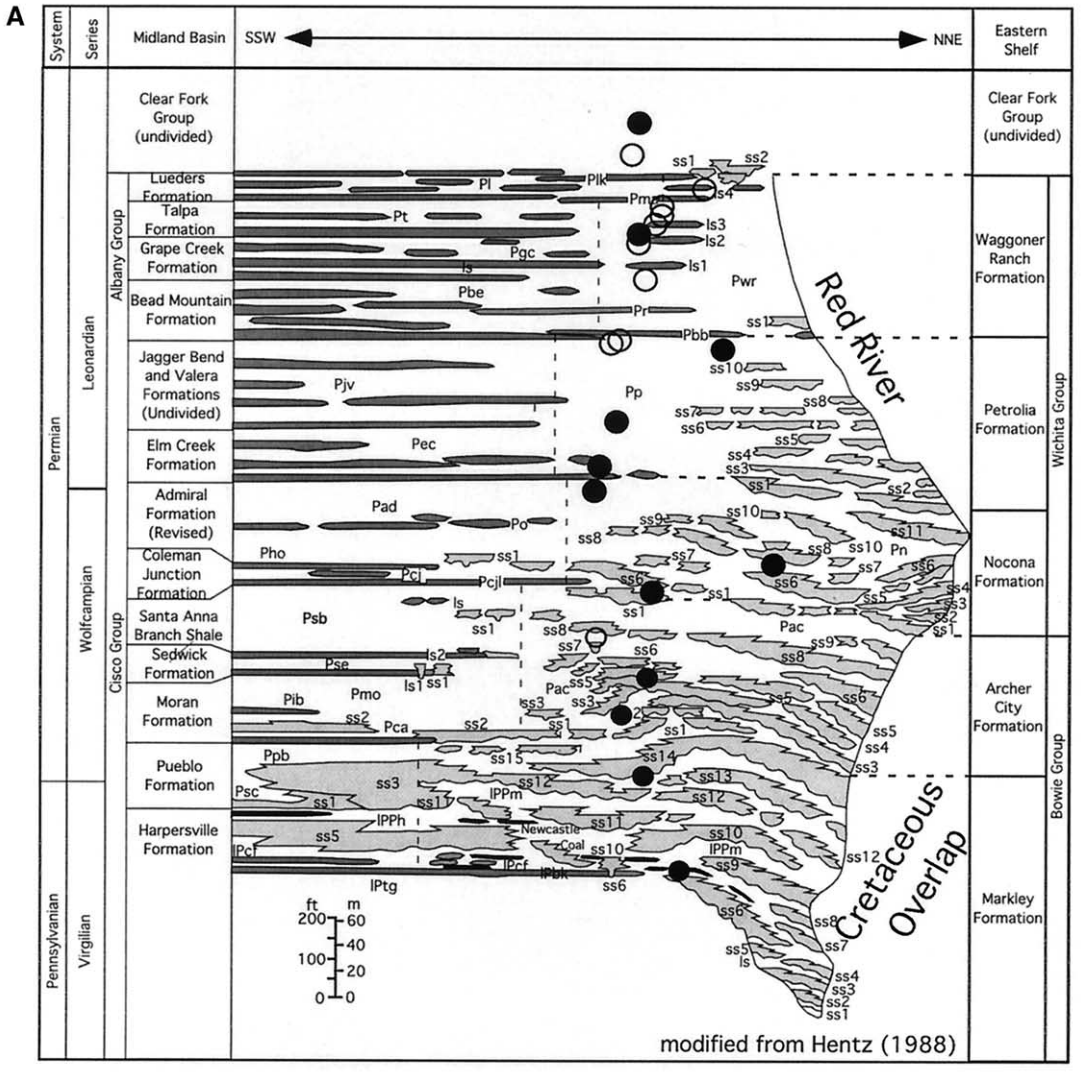
A
System
Series
Midland Basin
SSW
NNE
Eastern Shelf
Permian
Pennsylvanian
Leonardian
Wolfcampian
Virgilian
Albany Group
Cisco Group
Wichita Group
Bowie Group
Clear Fork Group (undivided)
Leuders Formation
Talpa Formation
Grape Creek Formation
Bead Mountain Formation
Jagger Bend and Valera Formations (Undivided)
Elm Creek Formation
Admiral Formation (Revised)
Coleman Junction Formation
Santa Anna Branch Shale
Sedwick Formation
Moran Formation
Pueblo Formation
Harpersville Formation
Waggoner Ranch Formation
Petrolia Formation
Nocona Formation
Archer City Formation
Markley Formation
Red River
Cretaceous Overlap
ft
m
200
60
100
40
20
0
0
modified from Hentz (1988)
B
Cretaceous
K
Clear Fork Group
Pcf
Wichita/Albany Group
Leuders
Pl
Waggoner Ranch
Pwr
Petrolia
Pp
Nocona
Pn
Bowie/Cisco Group
Archer City
Pac
Markley
PPm
Thrifty-Graham
PPtg
Canyon Group
PPc
Permian
Pennsylvanian
99
98
34
33
Seymour
Pcf
Pwr
Pp
Pn
Pl
Pac
K
PPm
PPtg
PPc

sonality in precipitation coincident with the transition to drier conditions.

## 2. MATERIALS AND METHODS

### 2.1. Paleosol Pyllosilicates

Paleosols were logged and described in the field according to the methods of Retallack (1988). To avoid recent weathering products not associated with Permo-Pennsylvanian pedogenesis, outcrop faces were dug back minimally 60 cm to provide a fresh surface for describing and sampling the paleosols. Approximately 500 g of paleosol matrix was collected from each paleosol horizon and stored in either canvas or plastic bags. Bulk paleosol matrix samples were initially dispersed in deionized water and shaken overnight. Both the $<2$-$\mu$m and $<0.2$-$\mu$m size fractions were isolated from the bulk paleosol matrix by centrifugation. For X-ray diffraction (XRD) analysis of the $<2$-$\mu$m size fraction, clays were exchange-saturated with K or Mg on filter membranes and transferred to glass slides as oriented aggregates. Duplicate Mg-saturated clays were also prepared with glycerol. Oriented aggregates of all Mg treatments were analyzed at 25°C; the K-saturated treatments were analyzed at 25°C, 300°C, and 500°C after 2 h of heating at their respective temperatures. Step scan analyses were performed with a Diano 8500 X-ray diffractometer with CuK$\alpha$ radiation between 2 and 30° 2$\theta$ with a step size of 0.04° 2$\theta$ and count time of 1 s. Mineralogical composition of the samples was determined following the methods of Moore and Reynolds (1997).

The $<0.2$-$\mu$m size fraction was subsequently treated in a series of selective dissolution procedures to remove contaminants that may complicate interpretation of $\delta^{18}$O values. Chemical pretreatments were, in the order of application, as follows: (1) 0.5 mol/L NaAOc to remove carbonates (Savin and Epstein, 1970; Lawrence and Taylor, 1971), (2) sodium hypochlorite (Clorox) solution (100°C, 1 h) buffered at pH 9.0 to remove occluded organic matter (Anderson, 1963), and (3) sodium citrate–bicarbonate–dithionite solution (80°C) to remove admixed secondary iron oxyhydroxides (Jackson, 1979). The $<0.2$-$\mu$m fraction was isolated from the bulk material for chemical and isotopic analysis given that previous work has shown authigenic clays dominate the $<0.2$-$\mu$m fraction (cf. Stern et al., 1997). XRD analyses of the $<0.2$-$\mu$m phyllosilicate fraction was performed in the same manner as described for the $<2$-$\mu$m fraction.

The $<0.2$-$\mu$m size fraction was split into two aliquots for chemical and stable isotope analysis. The first of these two aliquots was fused into a glass at high temperature (~1200°C) on molybdenum strips in an Ar atmosphere following the methods of Brown (1977). Samples were analyzed for major and minor elemental compositions with a Cameca SX 50 microprobe in the Department of Geology at the University of California–Davis. It is important to note that all of the phyllosilicate samples were stored in 2 M NaCl solution and subsequently washed to remove excess NaCl before chemical analysis, so all of the exchange sites in these phyllosilicates should be occupied by $Na^+$ and furthermore should be reflected in the elemental chemical data. The second aliquot of the $<0.2$-$\mu$m fraction was analyzed for $\delta^{18}$O with $BrF_5$ at ~560°C following the methods of Clayton and Mayeda (1963). Analysis was carried out on a Finigan MAT Delta E mass spectrometer in the Department of Geology at the Southern Methodist University. Oxygen isotopic compositions are reported relative to the Vienna standard mean ocean water (VSMOW) standard (Gonfiantini, 1984) with an analytical uncertainty, based on replicate analyses of samples and quartz standard NBS 28, of ± 0.2‰.

### 2.2. Paleosol Carbonates

Carbonates were collected near the base of each pedogenic carbonate horizon within paleosols. Doubly polished thin sections were analyzed petrographically to differentiate pedogenic carbonate fabrics from diagenetic calcite cements (Deutz et al., 2001). Microsamples were obtained from pedogenic micrite in carbonate nodules and rhizoliths; replacement of micrite and microspar or sparry calcite cements was avoided. Samples were drilled from thin sections or matching billets with a hand-held dental drill equipped with faceted 100-$\mu$m diamond bits. Approximately 50 $\mu$g of carbonate powder were roasted at 375°C for 3 h to remove organics. $\delta^{13}$C and $\delta^{18}$O analysis was carried out on a Fisons-Optima infrared gas source mass spectrometer in the Department of Geology at UC Davis. Carbonate isotope values are given relative to the standard PDB (Craig 1957) and interpreted meteoric water values are given relative to the standard VSMOW (Gonfiantini, 1984). Replicate analysis of NBS 19 yielded $\delta^{18}$O values of $-2.07 \pm 0.15$ ($n = 39$) over the period of analysis.

### 2.3. Soil Phyllosilicates

As a means of comparing phyllosilicates in a modern soil profile with those contained in the studied Permo-Pennsylvanian paleosols, we separated and analyzed by XRD the $<2$-$\mu$m fraction from a soil sampled in Butte County in the northern Sierra Nevada foothills of California. Similar methods of separation and chemical treatment for phyllosilicates in the Permo-Pennsylvanian paleosols were applied to the collection of the $<2$-$\mu$m fraction in this soil. This soil is classified as a fine-loamy, mixed, superactive, thermic Ultic Haploxeralf (refer to Soil Survey Staff, 1998). These soils occur at an elevation of 400 m, on a 12% slope that receives 1000 mm mean annual precipitation. The profile is underlain by quartz diorite and the vegetation is mostly blue oak (*Quercus douglasii*), interior live oak (*Quercus wiglizenii*), and annual grasses.

## 3. RESULTS

### 3.1. Phyllosilicate Mineralogy and Stratigraphic Distribution

There are two distinctly different suites of phyllosilicate minerals in the paleosol profiles; the stratigraphic separation between the two suites is just below the Permo-Pennsylvanian boundary. The majority of $<2$-$\mu$m size fraction samples from upper Pennsylvanian paleosol profiles exhibit sharp and intense 7 Å XRD peaks (Fig. 3). These peaks decompose upon K saturation and heating to 500°C, indicating the dominance of kaolinite. In addition, there is a relatively minor and broad XRD peak at 13 to 15 Å that is unaffected by Mg saturation and glycerol treatment. This peak could be either very fine grained vermiculite or an hydroxy-interlayered 2:1 mineral (the general category of these minerals is referred to as HIM) of unknown identity. Finally, a minor but persistent peak or "shoulder" at 10 Å indicates the presence of weathered mica such as biotite or muscovite.

Samples of the $<2$-$\mu$m and $<0.2$-$\mu$m size fractions of phyllosilicates from the uppermost Pennsylvanian through Lower Permian paleosols exhibit a distinctly different pattern of XRD peaks from similar size fractions in the older Upper Pennsylvanian paleosols. Although the 7- and 3.5-Å peaks are also present in the X-ray diffractograms of lower Permian paleosols (Figs. 4, 5), their relative intensities are much lower than equivalent peaks in the older upper Pennsylvanian samples (Fig. 3). In addition, the 13- to 15.5-Å peaks are of increased intensity relative to the Pennsylvanian phyllosilicates, indicating that smectite, rather than kaolinite, dominates the phyllosilicate mineralogy in the Lower Permian paleosols (Figs. 4, 5). Furthermore, some of these smectites do not collapse, or only partially collapsed, to 10 Å upon K saturation and heating to 550°C (Figs. 4, 5), suggesting that the interlayer spaces of these phyllosilicates are filled, thereby preventing collapse, and therefore indicates the presence of HIM. A 14- to 15-Å Mg-saturated peak present in many samples shifts to 17.5 to 18 Å upon treatment with glycerol (Fig. 4), further confirming the presence of smectite in Lower Permian paleosols.

A minor but persistent peak or shoulder at 10 Å indicates the

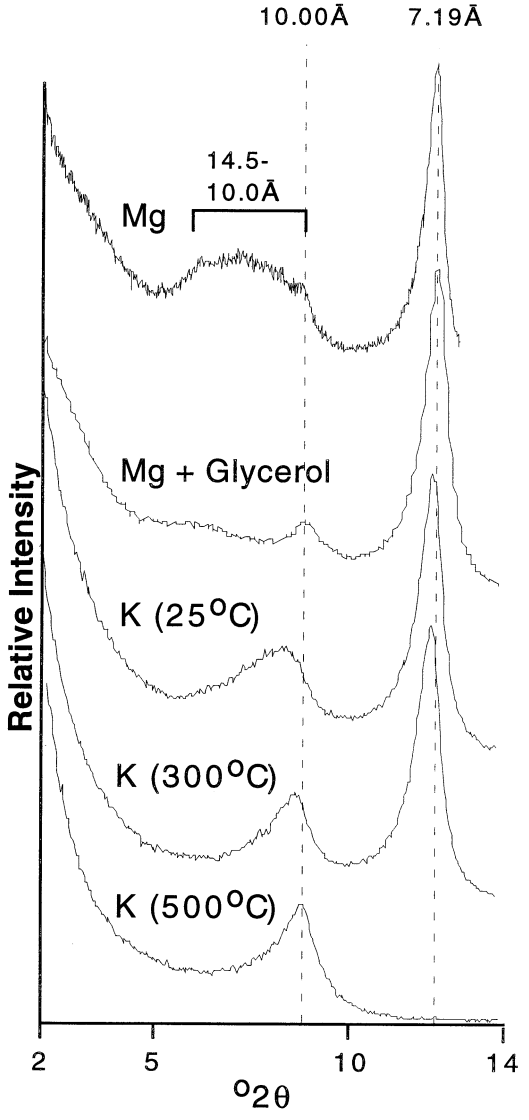


Fig. 3. XRD patterns of oriented <2-$\mu$m size fraction from the B-horizon of a paleosol beneath fluvial marker bed SS9 in the Upper Pennsylvanian Markley Formation. This particular sample is dominated by kaolinite. See text for explanation.

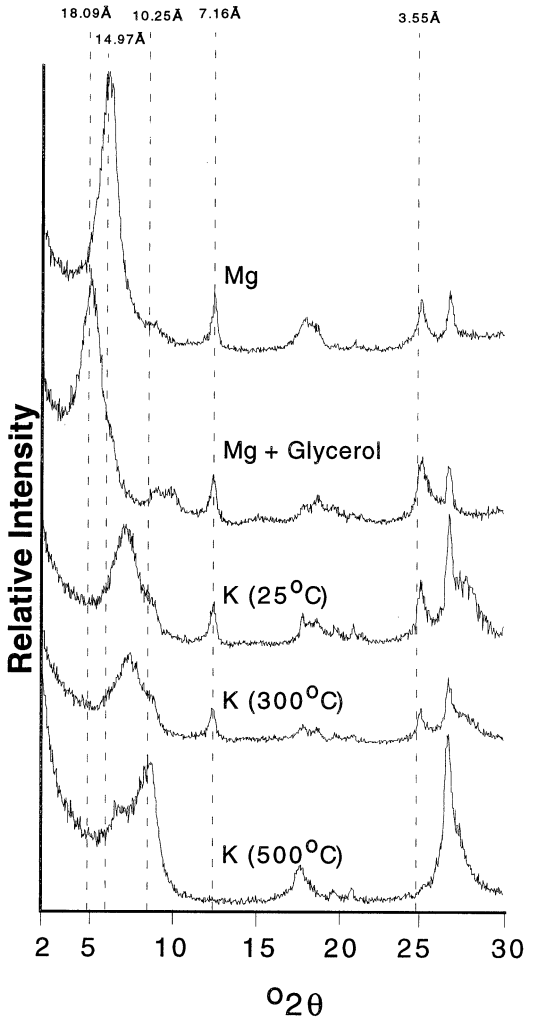


Fig. 4. XRD patterns of oriented <2-$\mu$m particle size fraction from the B-horizon of a paleosol beneath fluvial marker bed SS8 in the Early Permian Petrolia Formation. The text suggests this sample is dominated by smectite. See text for explanation.

minor occurrence of a weathered mica mineral in most of the B-horizons of both Late Pennsylvanian and Early Permian samples (Figs. 3–7). This phase is probably a relict detrital phase because there is no characteristic XRD evidence for diagenetic illitization of the <0.2-$\mu$m size fraction such as illite–smectite superstructures or stable ordering of illite and smectite layers within the same crystal lattice (Moore and Reynolds, 1997).

### 3.2. Distribution of Phyllosilicates within Paleosol and Soil Profiles

Systematic intraprofile variation in the relative proportion of phyllosilicate minerals is observed throughout each of the Upper Pennsylvanian and Lower Permian paleosols. In each paleosol profile the 7-Å kaolinite peak decreases in intensity downward from the interpreted paleosol surface (Figs. 6, 7). In several of the Lower Permian paleosol profiles the relative proportion of HIM increases in the upper horizons of the paleosol profile, as indicated by their greater intensity of the 14-Å peak (Fig. 7). Early Permian paleosol profiles also exhibit a broadening of the expandable 2:1 phyllosilicate (001) 14 to 18 Å peak, which increases the breadth of the (001) peak upward through the profile (Fig. 7). This broadening may be attributable to a number of factors such as crystal size and crystal defects, variable isomorphic substitution, or nonpreferred grain orientation as a result of intercalated organics that may not have been entirely removed by Na-hypochlorite treatment. This effect is similar to observations made in many modern soils (Fig. 8; Frye et al., 1968; Moore and Reynolds, 1997; Wilson, 1999). Moreover, in many of the paleosol profiles the smectite peak at 17 to 18 Å and the HIM (001) peak at 14 to 16 Å exhibit increasing intensity upward through the profile at the expense of the 10-Å weathered mica minerals (001) (Fig. 7). X-ray diffractograms of the modern soil from

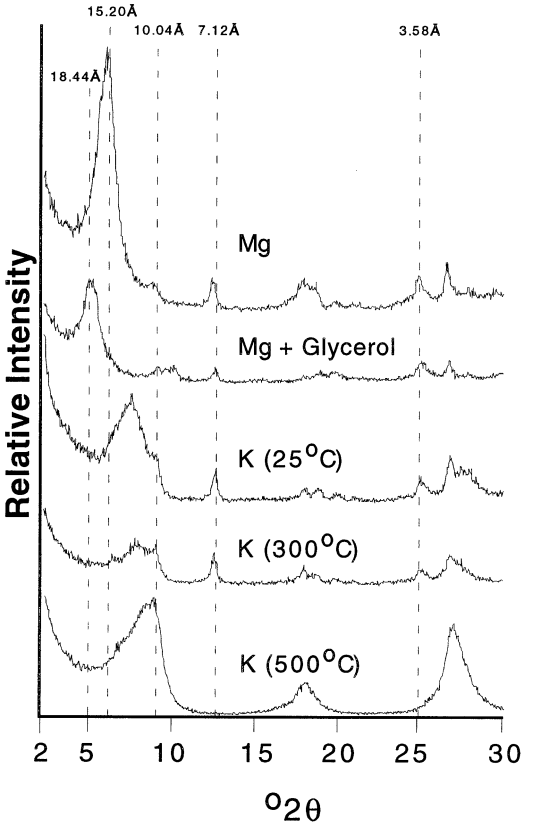


Fig. 5. XRD patterns of oriented <0.2-$\mu$m size fraction from the B-horizon of a paleosol between marine limestone marker beds ls3 and ls2 in the Early Permian Waggoner Ranch Formation. The sample is dominated by smectite with some hydroxy-interlayered minerals.

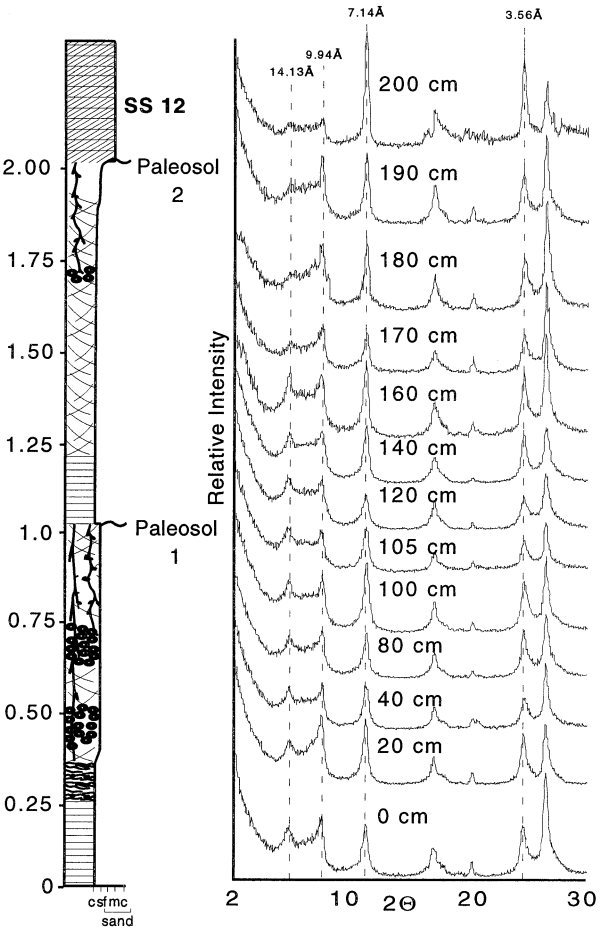


Fig. 6. Down-profile XRD patterns of Mg-saturated clays from the <2-$\mu$m size fraction of two paleosols underlying the SS12 marker bed in the Late Pennsylvanian Markley Formation. Measured section to the left shows stacked paleosols. Paleosol tops are indicated by wavy lines. Symbols are as follows: Fe-oxides = half-filled ovals; pedogenic slickensides = arcuate lines; rooting structures = vermicular patterns; C = clay; S = silt; f, m, c = fine, medium, and coarse sand. The XRD patterns demonstrate the increase up-profile in the relative intensity of the kaolinite (001) peak (7 Å) through the two paleosols.

California (Fig. 8) exhibit patterns similar to those observed in the Permian paleosol profiles. These trends include an increase in the down-profile intensity of the smectite (001) 18.5 Å peak at the expense of the 10-Å mica peak as well as increased intensity of the halloysite (001) 7.4 Å peak near the surface of the profile (Fig. 8). This trend in modern soils is interpreted to be a result of more intense weathering of primary minerals upward through the profile. By analogy, similar down-profile trends observed in the mineralogy of the Pennsylvanian and Permian paleosols is inferred to record pedogenic alteration of detrital micaceous minerals to authigenic kaolinite, HIM, and smectite. Finally, although XRD patterns reveal that quartz and weathered micas are largely absent from the <0.2-$\mu$m Permo-Pennsylvanian size fractions, their mineralogy is remarkably similar to the corresponding <2-$\mu$m size fraction.

### 3.3. Elemental Composition of the <0.2-$\mu$m Size Fraction

Table 1 lists the elemental composition of the <0.2-$\mu$m fraction from paleosol B-horizons. The <0.2-$\mu$m phyllosilicate fraction was used for chemical and stable isotope analysis because other workers have demonstrated that this size fraction in soils and paleosols is dominated by an authigenic phase (Stern et al., 1997). A mass balance of mineral components was not made because the concentration of individual phyllosilicate minerals within these mixtures cannot be directly measured by XRD. However, the chemical composition of these phyllosilicate mixtures provides insight to the relative concentration of certain minerals and allows for evaluation of stratigraphic trends.

There is an apparent temporal trend of increasing Si/Al ratios in the <0.2-$\mu$m pedogenic phyllosilicate fraction from average Si/Al ratios of 0.88 in the Late Pennsylvanian to 1.05 in the Early Permian samples. Relatively low potassium ($K_2O$) concentrations likely reflects the minor component of detrital weathered micas, indicated by the 10-Å (001) peaks observed in B-horizon XRD patterns. Sodium ($Na_2O$) likely reflects the presence of $Na^+$ in 2:1 exchange sites of expansible phyllosilicates, which were chemically pretreated to occupy 2:1 phyllosilicate exchange sites with $Na^+$. Sodium is not likely to occur in structural sites other than interlayer exchangeable sites. In this regard, the elemental chemical data reconfirms conclusions made from XRD data: the Pennsylvanian samples are dominated by kaolinite with extremely low cation exchange

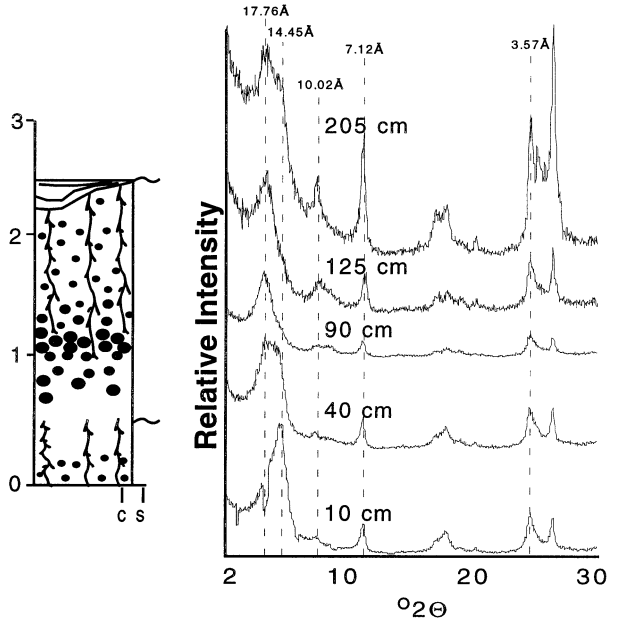


Fig. 7. Down-profile XRD patterns of Mg-saturated and glycerol-solvated clays in the <2-$\mu$m size fraction from a paleosol underlying SS7 of the Early Permian Petrolia Formation. Symbols are as follows: Paleosol top = wavy line; Fe-oxides = half-filled ovals; pedogenic slickensides = arcuate lines; rooting structures = vermicular patterns; C = clay; S = silt; f, m, c = fine, medium, and coarse sand. The XRD patterns indicate a down-profile decrease in the relative intensity and breadth of the hydroxy-interlayered 2:1 mineral (001) peak at 14 Å.

capacity, the Permian samples are dominated by smectite with much higher exchange capacity, and all of the samples contain a minor fraction of detrital mica. No other trends in cation ratios were observed.

### 3.4. $\delta^{18}$O values of Pedogenic Phyllosilicates and Carbonates

Table 2 and Figure 9 present the $\delta^{18}$O values of pedogenic calcites (n = 114) and phyllosilicates in the <0.2-$\mu$m size fraction (n = 12) from the paleosols. The $\delta^{18}$O values of pedogenic calcites are presented as the mean value, $\pm 1\sigma$, for individual paleosol profiles or compound sets of paleosol profiles that represent no more than 10 m of stratigraphic thickness (except for the Leuders Formation, which is 20 m thick). The $\delta^{18}O_{PDB}$ values of pedogenic carbonate show a range of ~5.4‰ from the most depleted values of −4.0‰ (26.8‰$_{SMOW}$) in the lower Nocona Formation (Wolfcampian) to the most enriched values of +1.4‰ (32.4‰$_{SMOW}$) in the upper Petrolia Formation (Leonardian; Fig. 9). Moreover, the $\delta^{18}O_{PDB}$ values of pedogenic calcites exhibit a generally progressive enrichment from the oldest Wolfcampian carbonate-bearing paleosols in the study area to stratigraphically higher and younger Leonardian paleosols. Superimposed upon the long-term increase in $\delta^{18}$O values are several shorter-term shifts of ~2.0 to 4.0‰ (Fig. 9).

The $\delta^{18}O_{SMOW}$ values of pedogenic phyllosilicate minerals range from ~19.6‰ in the upper Pennsylvanian and lowest Permian (Archer City Formation) paleosols to values as enriched as ~22.7‰ in the lower Permian (Leonardian) paleosols (Table 2; Fig. 9). The phyllosilicate $\delta^{18}$O values, however, do not reveal short-term isotopic fluctuations analogous to those defined by the $\delta^{18}$O values of pedogenic carbonates. However, there is a relatively abrupt shift in the $\delta^{18}$O composition of the phyllosilicates near the Pennsylvanian–Permian boundary (Fig. 9) from ~19.5 to 20.5‰ in the Pennsylvanian to 20.8 to 22.7‰ in the Early Permian. The observed oxygen isotope fractionation between penecontemporaneously formed calcite and

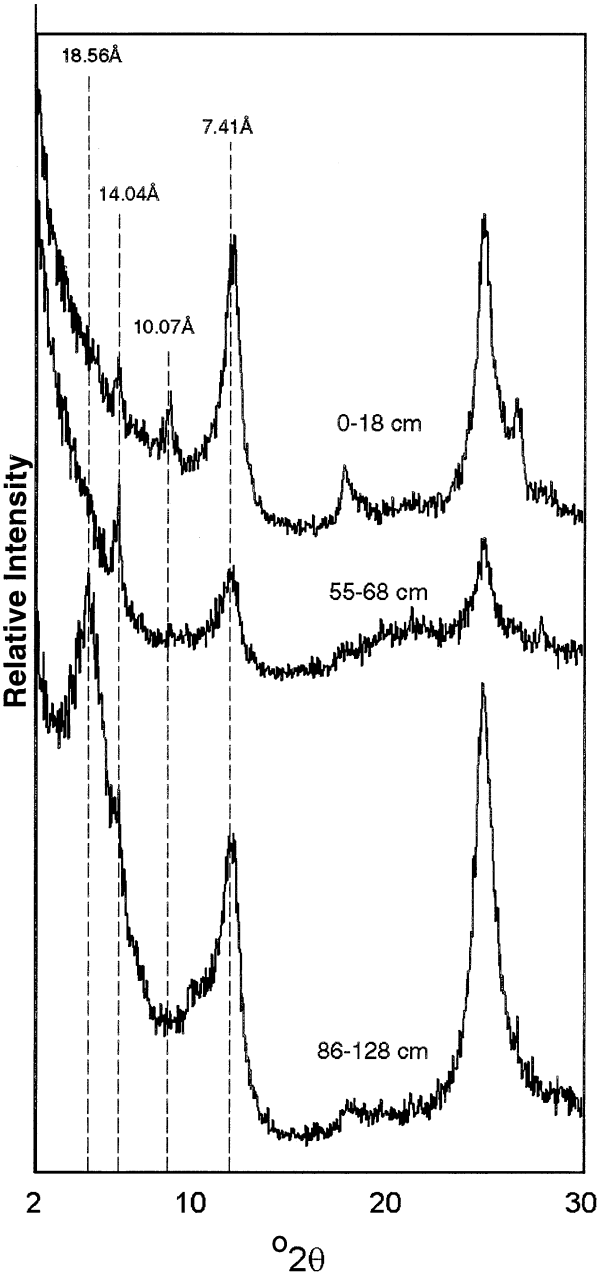


Fig. 8. Down-profile XRD patterns of Mg-saturated and glycerol-solvated clays in the <2-$\mu$m size fraction from the modern soil. The patterns show a down-profile decrease in the relative intensity of the 14-Å (001) HIM peak and an increase of the 18.5 Å-(001) smectite peak, and a down-profile decrease in the relative intensity of the 7.4-Å halloysite peak.

Table 1. Electron microprobe data for selected Permi-Pennsylvanian phyllosilicates.[a]

| Sample | Age | Formation | $Na_2O$[b] | MgO | $Al_2O_3$ | $SiO_2$ | $P_2O_5$ | $K_2O$ | CaO | $TiO_2$ | $MnO_2$ | $Fe_2O_3$ | SrO | Total | Si/Al |
|---|---|---|---|---|---|---|---|---|---|---|---|---|---|---|---|
| 1 | Virgilian | Markley (middle) | 0.66 | 0.58 | 31.39 | 62.65 | 0.03 | 1.66 | 0.06 | 0.97 | 0.03 | 1.94 | 0.23 | 100.19 | 1.04 |
| 2 | Virgilian | Markley (upper) | 0.79 | 0.82 | 36.83 | 54.17 | 0.06 | 1.66 | 0.09 | 0.73 | 0.01 | 2.73 | 0.22 | 98.12 | 0.77 |
| 3 | Virgilian | Markley (upper) | 8.35 | 0.95 | 34.06 | 54.92 | 0.05 | 0.60 | 0.02 | 0.34 | 0.02 | 1.20 | 0.22 | 100.73 | 0.84 |
| 4 | Wolfcampian | Archer City (lower) | 6.67 | 4.22 | 26.03 | 56.49 | 0.07 | 1.03 | 0.24 | 0.78 | 0.04 | 5.44 | 0.25 | 101.24 | 1.13 |
| 5 | Wolfcampian | Archer City (middle) | 6.88 | 1.90 | 30.99 | 56.16 | 0.02 | 0.76 | 0.03 | 0.36 | 0.03 | 3.82 | 0.22 | 101.17 | 0.94 |
| 6 | Wolfcampian | Nocona (lower) | 2.78 | 2.54 | 29.35 | 55.04 | 0.04 | 3.56 | 0.02 | 0.56 | 0.02 | 5.49 | 0.25 | 99.67 | 0.98 |
| 7 | Wolfcampian | Nocona (middle) | 4.98 | 2.50 | 24.34 | 57.91 | 0.03 | 2.06 | 0.03 | 0.73 | 0.02 | 7.38 | 0.23 | 100.20 | 1.24 |
| 8 | Wolfcampian | Nocona (upper) | 5.58 | 3.32 | 27.57 | 55.81 | 0.04 | 1.96 | 0.04 | 0.37 | 0.02 | 5.23 | 0.22 | 100.16 | 1.05 |
| 9 | Leonardian | Petrolia (lower) | 2.74 | 2.84 | 29.58 | 55.22 | 0.03 | 3.08 | 0.02 | 0.41 | 0.03 | 5.27 | 0.23 | 99.44 | 0.97 |
| 10 | Leonardian | Petrolia (middle) | 5.93 | 3.68 | 28.91 | 55.82 | 0.02 | 0.81 | 0.05 | 0.46 | 0.02 | 4.86 | 0.23 | 100.79 | 1.00 |
| 11 | Leonardian | Waggonner Ranch (upper) | 4.60 | 4.01 | 26.25 | 56.82 | 0.02 | 1.87 | 0.03 | 0.58 | 0.03 | 5.96 | 0.25 | 100.42 | 1.12 |
| 12 | Leonardian | Clear Fork (lower) | 2.42 | 3.49 | 28.71 | 54.60 | 0.03 | 4.53 | 0.01 | 0.30 | 0.02 | 5.37 | 0.23 | 99.71 | 0.99 |

[a] Chemical data are presented as the mean of 15 data individual analyses for each sample.
[b] Sodium data are the least reliable values using this technique (Brown, 1977). However, the maximum standard deviation for $Na_2O$ is 0.53 wt % for sample 10, the minimum standard deviation is 0.10 wt % for sample 8, and the mean standard deviation for $Na_2O$ in all sample is 0.22 wt %.

smectite (presented as $\Delta^{18}O_{SMOWphyllo\text{-}carb}$ in Table 2) varies from 4.6‰ to 9.7‰.

## 4. DISCUSSION

### 4.1. Diagenesis

To infer paleoenvironmental and paleoclimatic conditions from the mineralogical, chemical, and isotopic composition of paleopedogenic minerals, it must be demonstrated that their compositions have not been diagenetically altered. Maximum burial temperatures to which Permo-Pennsylvanian strata of the eastern shelf of the Midland Basin were exposed are likely $<$ 50°C (Ruppel and Hovorka, 1995). Furthermore, phyllosilicates in the $<0.2$-$\mu$m size fraction from these paleosol profiles exhibit mineralogical trends that are analogous to those observed in modern soil profiles, such as a decrease in the proportion of 2:1 expandable phyllosilicates and kaolinite and an increase in 2:1 nonexpandable phyllosilicates downward within individual profiles. Finally, the $\delta^{18}O$ values of pedogenic phyllosilicates and calcites exhibit a similar stratigraphic pattern relative to one another. This pattern would not be expected if diagenesis had played an active role in the alteration

Table 2. $\delta^{18}O$ data for pedogenic calcite and phyllosilicates from Permi-Pennsylvanian paleosols.

| Formation | Meters[a] | $\delta^{18}Ophyllo_{SMOW}$ | $\delta^{18}Occ_{PDB}$ | $\delta^{18}Occ_{SMOW}$ | $\Delta^{18}O_{smow\ phyllo.\text{-}carb}$[b] |
|---|---|---|---|---|---|
| Markley | 135 | 20.5[1] | — | — | 6.6 |
| Markley | 180 | 19.6[2] | — | — | 7.5 |
| Archer City | 230 | 19.5[3] | — | — | 7.6 |
| Archer City | 265 | 20.8[4] | $-3.7 \pm 0.4$, n = 4 | $27.1 \pm 0.4$, n = 4 | 6.3 |
| Archer City | 315 | — | $-2.9 \pm 0.4$, n = 4 | $27.9 \pm 0.4$, n = 4 | |
| Nocona | 325 | 21.1[5] | $-4.0 \pm 0.0$, n = 1 | $26.8 \pm 0.0$, n = 1 | 5.7 |
| Nocona | 365 | 21.1[6] | $-2.6 \pm 0.2$, n = 3 | $28.2 \pm 0.2$, n = 3 | 7.1 |
| Nocona | 395 | 21.8[7] | $-1.0 \pm 1.0$, n = 9 | $29.9 \pm 1.0$, n = 9 | 8.1 |
| Petrolia | 415 | 21.2[8] | $0.0 \pm 0.4$, n = 7 | $30.9 \pm 0.4$, n = 7 | 9.7 |
| Petrolia | 475 | 22.7[9] | $-3.5 \pm 0.4$, n = 10 | $27.3 \pm 0.4$, n = 10 | 4.6 |
| Petrolia | 525 | 21.1[10] | $-2.5 \pm 0.3$, n = 7 | $28.3 \pm 0.3$, n = 7 | 7.2 |
| Petrolia | 535 | — | $1.0 \pm 0.8$, n = 6 | $31.9 \pm 0.8$, n = 6 | |
| Petrolia | 538 | — | $1.4 \pm 0.4$, n = 4 | $32.4 \pm 0.4$, n = 4 | |
| Wagoner Ranch | 585 | — | $-1.3 \pm 1.7$, n = 8 | $29.6 \pm 1.7$, n = 8 | |
| Wagoner Ranch | 615 | — | $0.6 \pm 0.2$, n = 2 | $31.5 \pm 0.2$, n = 2 | |
| Wagoner Ranch | 620 | 22.6[11] | $0.5 \pm 0.4$, n = 2 | $31.4 \pm 0.4$, n = 2 | 8.8 |
| Wagoner Ranch | 625 | — | $0.8 \pm 0.6$, n = 4 | $31.7 \pm 0.6$, n = 4 | |
| Wagoner Ranch | 630 | — | $1.0 \pm 0.2$, n = 4 | $31.9 \pm 0.2$, n = 4 | |
| Wagoner Ranch | 635 | — | $1.1 \pm 1.0$, n = 2 | $32.0 \pm 1.0$, n = 2 | |
| Lueders | 645 | — | $1.0 \pm 1.7$, n = 13 | $32.0 \pm 1.7$, n = 13 | |
| Clear Fork | 665 | — | $0.8 \pm 0.7$, n = 5 | $31.7 \pm 0.7$, n = 5 | |
| Clear Fork | 710 | 22.0[12] | $-3.0 \pm 0.5$, n = 6 | $27.8 \pm 0.5$, n = 6 | 5.8 |
| Clear Fork | 782 | — | $-1.2 \pm 0.8$, n = 4 | $29.7 \pm 0.8$, n = 4 | |
| Clear Fork | 840 | — | $0.9 \pm 0.6$, n = 5 | $31.8 \pm 0.6$, n = 5 | |

[a] Meter levels are calculated as the stratigraphic distance above the base of the Pennsylvanian Markley Formation.
[1-12] Numbers 1 to 12 correspond to phyllosilicate sample designations in Table 1 and Figure 10.
[b] The $\Delta^{18}O_{smow\ phyllo.\text{-}carb}$ values are calculated from the $\delta^{18}Ophyllo_{SMOW}$ and the average $\delta^{18}Occ_{SMOW}$ from each corresponding horizon. THe average $\delta^{18}Occ_{SMOW}$ value from horizon 4 was used to calculate $\Delta^{18}O_{smow\ phyllo.\text{-}carb}$ for horizons 1 to 3 because no calcite was found associated with these horizons.

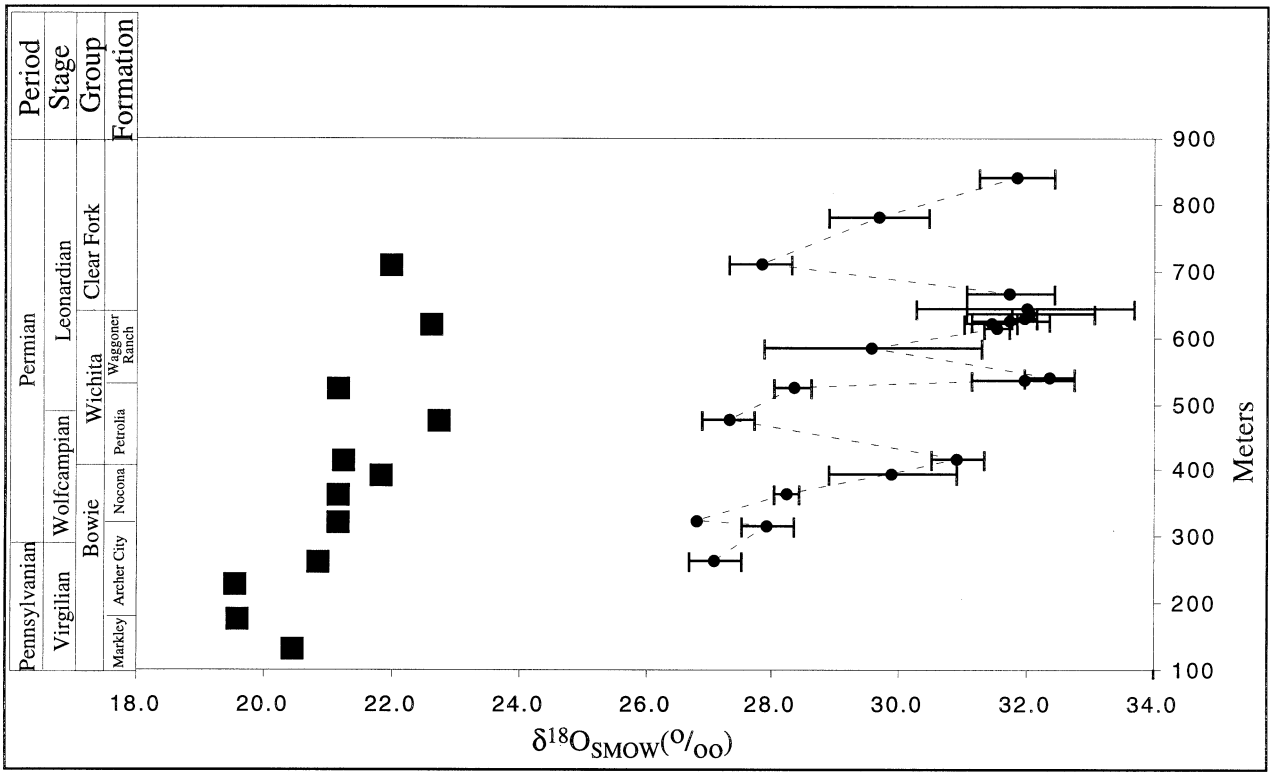


Fig. 9. Stratigraphic distribution of $\delta^{18}O$ values of pedogenic calcites and phyllosilicates. The mean calcite $\delta^{18}O_{SMOW}$ values (solid circles) increase from ~27‰ in the Lower Permian paleosols to ~32‰ in uppermost Lower Permian paleosols. The $\delta^{18}O$ values of phyllosilicates (solid squares) in the $<0.2$-$\mu$m size fraction increase from ~19.5‰ in Upper Pennsylvanian/lowermost Lower Permian paleosols to ~23‰ in the uppermost Lower Permian paleosols. The error bars represent $\pm 1\sigma$ for each calcite data point. Each mean $\delta^{18}O_{SMOW}$ calcite value is representative of individual paleosol profiles or compound sets of paleosols. The meter values on the right-hand axis are calculated as the stratigraphic thickness from the base of the Virgilian Markley Formation.

of these minerals because it is unlikely that smectite, kaolinite, and calcite would undergo similar amounts of oxygen isotope exchange during diagenesis as a result of their greatly differing chemical stability, solubility, and crystal sizes (Stern et al., 1997). We therefore conclude that diagenesis has minimally affected the phyllosilicate and carbonate mineralogy or their oxygen isotopic compositions.

### 4.2. Clay Mineralogy

Paleosols from the Upper Pennsylvanian and Lower Permian strata of north-central Texas exhibit changes in their clay mineralogy that are similar to trends observed in modern weathering profiles. The up-profile change in kaolinite content at the expense of detrital nonexpandable 2:1 phyllosilicates (mica) coupled with increased broadening of the 2:1 phyllosilicate (001) peak seen within individual paleosols (Figs. 6, 7) is analogous to that observed in the modern soil profile and in previously studied soils (Frye et al., 1968; Wilson, 1999). These results support the hypothesis of a dominantly pedogenic origin for the phyllosilicates in the $<0.2$-$\mu$m size fraction of the Pennsylvanian and Permian paleosols. The long-term trend in paleosol B-horizon mineralogy from kaolinite dominated to smectite dominated, in conjunction with an increase in Si/Al ratios from Upper Pennsylvanian to Lower Permian phyllosilicates, suggests a shift from relatively humid to semiarid and seasonal climatic conditions during this time period. These results thus corroborate a paleoclimate trend of a progressive shift to increased aridity previously delineated from paleosol morphologies (Tabor and Montanez, personal communication).

Although there is some evidence for kaolinite genesis in cold and wet climates (Bird and Chivas, 1989), kaolinite formation in soil profiles is typically associated with intense weathering of stable landscapes under warm, humid conditions (Chamley, 1989; Wilson, 1999). The dominance of kaolinite in upper Pennsylvanian paleosols is thus interpreted to reflect pedogenesis under warm humid climate conditions. In contrast, vermiculite and HIV are typically found in well-drained soil profiles within subtropical and temperate zones (April et al., 1986; Bain et al., 1990; Moore and Reynolds, 1997; Wilson, 1999). Although these 2:1 phyllosilicates occur as an auxiliary mineral phase in some tropical soils (Moniz et al., 1982), they generally do not occur in modern humid tropical soils, given that intense chemical weathering often results in direct transformation of micas to kaolinite (Wilson, 1999). The presence of HIM in Lower Permian paleosols likely records decreased soil moisture conditions in the Early Permian, conditions entirely consistent with a trend toward more dry and arid conditions (Tabor and Montanez, personal communication).

The presence of pedogenic smectite in these Early Permian paleosols is compatible with formation under tropical or subtropical conditions, but only if soils formed in poorly drained landscapes or under a seasonal (e.g., monsoonal) climate. Formation of smectite is typically associated with soils that develop in low-lying topography, with poor drainage and base-rich parent material, leading to favorable chemical conditions characterized by high pH, high silica activity and an abundance of basic cations. These conditions would be typical of floodplain environments in virtually all temperate and many tropical climates with a naturally high water table (Allen and Hajek, 1989). However, most of the studied soils probably were not poorly drained in the Early Permian, given that paleosol morphologies are characterized by well developed soil structure, extensive rooting systems and colors that are consistent with well drained modern soils (Tabor and Montanez, personal communication). These results indicate a mineralogical suite that is consistent with humid tropical settings in the Late Pennsylvanian changing to a subhumid to semiarid seasonal, or monsoonal, climatic setting by early Permian time.

### 4.3. Mineral and Meteoric Water Isotope Systematics

The isotopic composition of precipitation and meteoric water has been shown to vary systematically with geographic position (Dansgaard, 1964; Rozanski et al., 1993). Thus, the natural range of oxygen isotope values in modern precipitation varies from ~0‰ to −40‰. This large range of values reflects the effects of Rayleigh distillation during progressive rainout over continental interiors and highlands. The isotopic composition of coastal precipitation averages ~0‰, reflecting minimal Rayleigh distillation. More depleted $\delta^{18}O$ values are found in continental interiors and high latitudes as a result of progressive rainout of $^{18}O$ from the original air mass. Highly depleted meteoric water values ($\leq -10$‰) in tropical and midlatitudes may also reflect a significant loss of water vapor from clouds as weather systems pass over prominent orographic features such as the present-day Cordilleran system and the Himalayan–Tibetan Plateau of central Asia (Rozanski et al., 1993; Sheppard, 1986). The isotopic composition of first-formed water vapor in a cloud, however, will reflect the isotopic composition of seawater. Therefore, the effect of fluctuations in the $\delta^{18}O$ composition of seawater, of potentially up to 8‰ (Hudson and Anderson, 1989; Veizer, 1999), on the composition of meteoric water must be considered. However, others have argued that the $\delta^{18}O$ value of seawater may have remained at approximately 0‰ ± 2‰ throughout the Phanerozoic as a result of buffering by hydrothermal exchange at midocean ridges and continental weathering (Holland, 1984; Lecuyer and Allemand, 1999).

Pedogenic minerals inherit their oxygen isotope composition from soil water, which in turn can be correlated to the isotopic composition of meteoric precipitation (Savin and Epstein, 1970; Lawrence and Taylor, 1971; Hsieh, 1996; Savin and Hseih, 1998). The $\delta^{18}O$ of pedogenic phyllosilicates, Fe-oxyhydroxides, and carbonates exhibit a nearly 1:1 correlation with a consistent offset from the $\delta^{18}O$ composition of average local meteoric water (Lawrence and Taylor, 1971; Quade et al., 1989; Cerling and Quade, 1993; Yapp, 1993). However, soil water may undergo further isotopic fractionation as a result of evaporative enrichment or mineral weathering reactions within the soil profile leading to more enriched (>0‰) $\delta^{18}O$ compositions in both soil water and pedogenic minerals (Hsieh, 1996).

Furthermore, when comparing the $\delta^{18}O$ values of "contemporaneous" pedogenic minerals from individual soils or paleosols, one must account for the possibility that the soil minerals formed from soil waters whose $\delta^{18}O$ composition varied seasonally. Thus, the mineral pair may not exhibit the anticipated equilibrium per mil fractionation. The latter was demonstrated in the Miocene paleosols of the Siwalik Himalayan Molasse by Stern et al. (1997) where the oxygen isotopic composition of pedogenic smectite and calcite differed significantly because of formation under different soil moisture regimes. Smectite formed in these soils when conditions were wet enough to dissolve primary silicates, whereas calcite formed under soil-evaporative conditions associated with dry intervals.

### 4.4. $\delta^{18}O$ Compositions

We interpret the $\delta^{18}O$ values of the <0.2-$\mu$m clay fraction to record primarily pedogenic values given that (1) our $\delta^{18}O$ values for kaolinite samples (+19.6‰ and +20.5‰) from Upper Pennsylvanian paleosols are similar to previously published Upper Pennsylvanian paleopedogenic kaolinites from northern Texas (20.9‰ and 19.2‰; Lawrence and Rashkes Meaux, 1993); and (2) the clay mineralogical trends suggest that pedogenic phyllosilicates dominate the <0.2-$\mu$m fraction. Although the $\delta^{18}O$ values of the <0.2-$\mu$m pedogenic phyllosilicates and contemporaneous calcites record similar long-term trends throughout the Upper Pennsylvanian and Lower Permian stratigraphic interval, they define an oxygen isotope fractionation ($\Delta^{18}O_{SMOWphyllo\text{-}carb}$ in Table 2) that varies from calculated equilibrium fractionation values of <4‰ between smectite and coprecipitated calcite (Sheppard and Gilg, 1996; Kim and O'Neil, 1997; Stern et al., 1997). This apparent isotopic disequilibrium between these contemporaneous minerals may reflect a contribution from detrital phyllosilicate minerals of differing $^{18}O$ compositions, seasonal variation in the isotope composition of the soil water from which they precipitated, or both.

The presence of a small 10-Å peak on XRD graphs indicate that all of the <0.2-$\mu$m size phyllosilicate fraction from the paleosols contain a minor fraction of a detrital weathered mica. A minor component of mica can significantly alter the measured $\delta^{18}O$ composition of a heterogeneous phyllosilicate fraction (cf. Taylor and Sheppard, 1986; Sheppard and Gilg, 1996; Hoefs, 1997). Physical or chemical isolation of a phyllosilicate monomineralic fraction has proven to be difficult. If the relative contribution of oxygen from each mineral phase cannot be directly evaluated, then the interpretation of the stable isotope compositions of heterogeneous phyllosilicate fractions can be compromised. The issue is minimized, however, for mixes of kaolinite and smectite, such as those found in these paleosols, given that the temperature-dependent oxygen isotopic fractionation for these minerals is similar at Earth surface temperatures (Sheppard and Gilg, 1996). Micas (e.g., biotite or muscovite), however, have $\delta^{18}O$ compositions and $\delta^{18}O$ fractionation values that are significantly different from pedogenic clays such as smectite or kaolinite.

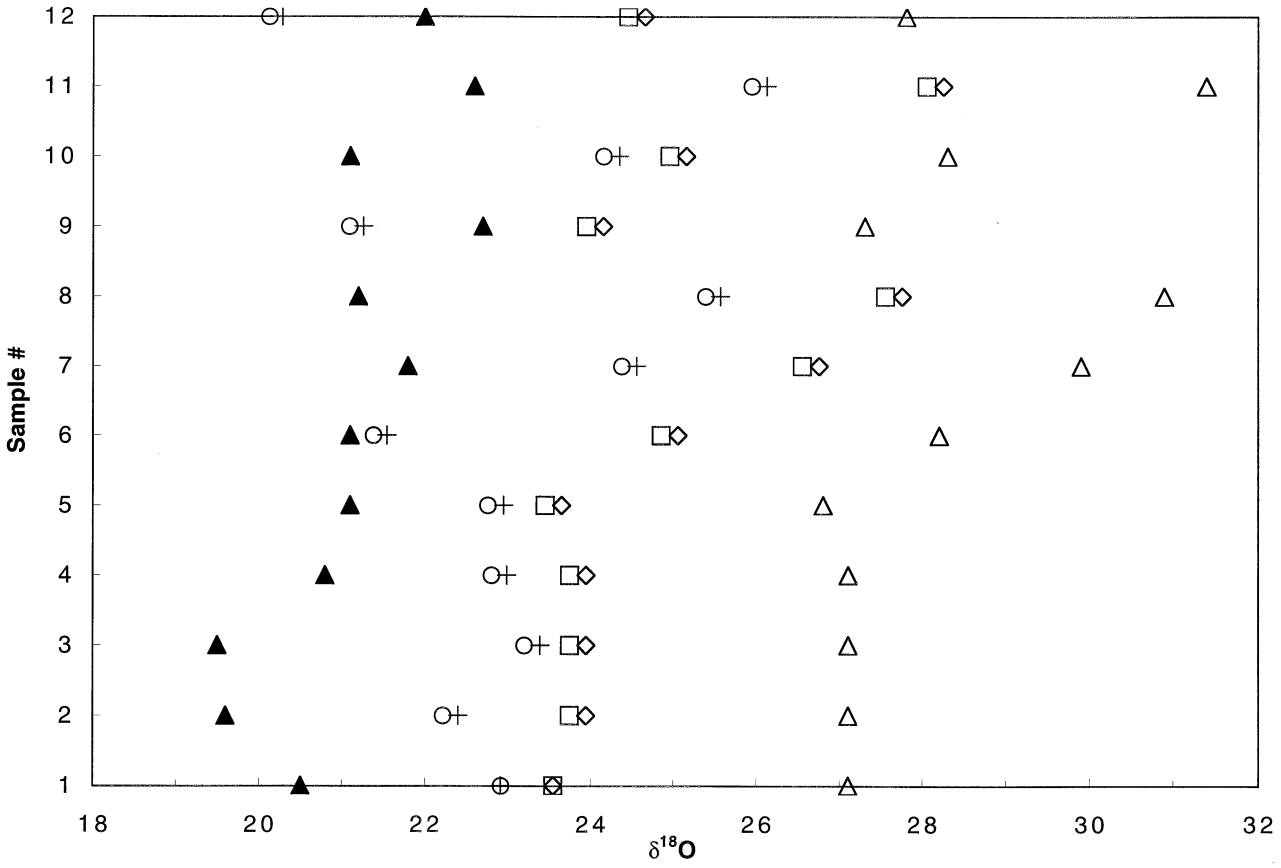


Fig. 10. $\delta^{18}O$ mixing model for measured and calculated pedogenic phyllosilicates and calcites. Sample numbers are from Tables 1 and 2. Average measured $\delta^{18}O$ values of pedogenic calcite (open triangles) plotted relative to $\delta^{18}O$ values of stratigraphically contemporaneous $<0.2$-$\mu$m phyllosilicates (solid triangles). Open squares and diamonds are calculated $\delta^{18}O$ values of a monomineralic nontronite that is in isotopic equilibrium with measured values of pedogenic calcite at 20° and 30°C. Open circles (20°C) and crosses (30°C) are calculated $\delta^{18}O$ values of a mixture of pedogenic nontronite and detrital biotite, which has a $\delta^{18}O = 5.5‰$. The amount of biotite within each sample mixture was estimated on the basis of the concentration of $K_2O$ of each sample (Table 1).

We developed a simple model to evaluate to what degree the observed oxygen isotopic disequilibrium between the phyllosilicate and calcite samples records the influence of detrital phyllosilicates and/or seasonal variation in soil water $\delta^{18}O$ composition (Fig. 10). The $\delta^{18}O$ composition of soil waters from which the pedogenic carbonates in the paleosols likely precipitated was calculated by using a tropical temperature range of 20 to 30°C and the empirically derived carbonate–water oxygen isotope fractionation of Kim and O'Neil (1997). By use of this estimated range of soil water $\delta^{18}O$ compositions, the $\delta^{18}O$ compositions of the monomineralic phyllosilicate component that would have precipitated from these waters was derived ("100% pedogenic" in Fig. 10). These estimates apply the thermodynamic equations of Sheppard and Gilg (1996) with a chemical composition equivalent to that of a sodium-saturated nontronite: $Na_{0.33}\ Fe_2Si_{3.67}Al_{0.33}O_{10}(OH)_2$. Nontronite is a reasonable phyllosilicate to select for this exercise because many modern soil-formed smectites are $Fe^{3+}$ rich and the elemental analysis of the fused minerals indicate a significant Fe content (Table 1).

The proportion of each sample made up of detrital micaceous minerals was calculated by assuming that all measured $K^+$ (reported in Table 1 as $K_2O$) occurs in a mica mineral such as biotite: $KMg_{1.5}\ Fe_{1.5}AlSi_3O_{10}(OH)_2$. Finally, the $\delta^{18}O$ composition of the synthetic mixture of pedogenic nontronite and detrital mica was calculated by using mass balance considerations and a $\delta^{18}O$ value of 5.5‰ for the detrital phase ("Biotite corrected" in Fig. 10; cf. Taylor, 1986; Hoefs, 1997). If the corrected values approach actual measured values then the apparent isotopic disequilibrium is likely attributable to the presence of allogenic micas rather than to climatic phenomena such as seasonality. It should be pointed out that extrapolation to end-member $\delta^{18}O$ values in these types of systems should use the mole fraction of oxygen from each constituent mineral phase, and not weight percent oxide (as reported in Table 1), as the compositional variable (cf. Yapp, 1990). However, both the calculated stoichiometric biotite and nontronite have nearly identical mole fractions of oxygen (0.45), and therefore the weight percent oxide will give equivalent $\delta^{18}O$ values to that of mole fraction.

Most of the calculated monomineralic $\delta^{18}O$ values of calculated mixtures of pedogenic and detrital phyllosilicate fractions show a shift from monomineralic pedogenic phyllosilicates toward the measured phyllosilicate $\delta^{18}O$ values (Fig. 10). This

suggests that the observed oxygen isotopic disequilibrium records in part the presence of detrital phyllosilicates. However, most of the biotite-corrected $\delta^{18}O$ values are still isotopically enriched by as much as 2 to 4‰ over the measured phyllosilicate samples relative to the $\delta^{18}O$ phyllosilicate values from the studied paleosols. It is possible that this "residual" isotopic enrichment reflects precipitation of the pedogenic phyllosilicates from soil waters that were $^{18}O$-depleted relative to carbonate-precipitating soil waters as a result of precipitation of these mineral suites during different seasons. In a study of contemporaneous pedogenic calcites and phyllosilicates from paleosols in the Miocene-age Himalayan Molasse, Stern et al. (1997) observed an oxygen isotopic fractionation between pedogenic calcites and smectites or kaolinites greater than would be expected (~4‰ enriched). They interpreted this isotopic enrichment over equilibrium fractionation values to record precipitation of the two pedogenic minerals from soil waters whose $\delta^{18}O$ values varied seasonally. Pedogenic calcite formed predominantly during the dry winter season, whereas phyllosilicates formed predominantly during the wet summer season. However, the observed isotopic offset between pedogenic phyllosilicates and calcites from the Permo-Pennsylvanian paleosols could alternatively reflect the presence of a currently unrecognized detrital or authigenic component with relatively low oxygen isotope values, such as aluminous hydrates or iron oxides that have not been completely removed by chemical pretreatment. Further analysis of these "pedogenic" phyllosilicates is clearly needed before more refined paleoclimate interpretations can be drawn from the $\delta^{18}O$ values of the fine-grained clay fraction in paleosols.

On the basis of the $\delta^{18}O$ values of the $<0.2$-$\mu$m size phyllosilicate fraction and contemporaneous pedogenic calcites, several significant paleoclimate conditions can be inferred through the Late Pennsylvanian through Early Permian. The long-term trend of isotopic enrichment defined by $\delta^{18}O$ values of phyllosilicates from 19.5‰$_{SMOW}$ to 22.7‰$_{SMOW}$ and $\delta^{18}O$ values of pedogenic calcites from ~27‰$_{SMOW}$ to ~32‰$_{SMOW}$ is consistent with a progressive increase in evaporation of soil water through this time period. This record corroborates a long-term climate trend toward increased aridity independently derived by using the macromorphologic features of the paleosols (Tabor and Montanez, personal communication). Estimates of paleotemperature or soil water composition are not possible given that these variables affect the $\delta^{18}O$ values of the measured calcite.

The observed shift in $\delta^{18}O$ values of pedogenic carbonates cannot be attributed to temperature change alone given that the observed 5‰ shift would require a corresponding change in paleotemperature of ~25°C. Although temperatures could have possibly been warmer (cf. Pearson et al., 2001), a first order assumption of an average surface temperature of 25°C is reasonable given that (1) northern Texas remained within the equatorial belt of Pangea throughout this geologic interval (Scotese, 1984; Parrish, 1993, 1995; Ziegler et al., 1996) and (2) the tropics maintain average temperatures within 1°C over extremely long timescales (Barron and Moore, 1994; Barron and Fawcett, 1995). If the shift in $\delta^{18}O$ values of pedogenic carbonates records solely a change in the $\delta^{18}O$ of soil waters through time, then soil water compositions varied from approximately −2‰ in the earliest Permian (Wolfcampian) to as high as +3.5‰ in the later part of the Early Permian (Leonardian). These soil water $\delta^{18}O$ compositions are consistent with near-coastal modern soil waters that have undergone evaporative enrichment in the soil profile (Cerling, 1984; Cerling and Quade, 1993; Rozanski et al., 1993). Perhaps the most significant result from this study is that these estimated soil waters would have required minimal rainout of precipitation from their source areas before entering the soil profiles. These results strongly suggest a proximal source of precipitation.

The presence of several shorter-term oscillations in $\delta^{18}O$ values of ~2 to 4‰ (Fig. 9), which may have occurred over $10^5$ to $10^6$-yr timescales and are superimposed on the long-term trend (~30 My), is interpreted to record changes in the intensity of soil leaching regimes (i.e., moist–more intense to dry–less intense). Short-term shifts in soil leaching regimes of similar temporal scale to those inferred from the $\delta^{18}O$ composition of the pedogenic minerals were previously and independently inferred from the stratigraphic distribution of polygenetic paleosols with anomalous positioning of carbonate-rich and clay-rich horizons (Tabor and Montanez, personal communication).

These estimated soil water $\delta^{18}O$ values from Late Pennsylvanian through Early Permian paleosols (and by inference, paleoprecipitation) for western equatorial Pangea, however, are inconsistent with current models of Early Permian paleoprecipitation and paleoatmospheric circulation patterns over Pangea. Precipitation over western equatorial Pangea is currently modeled to have been isotopically depleted as a result of the effects of extensive rainout as Tethys-sourced waters migrated over Pangea (Crowley et al., 1993; Parrish, 1993, 1995; Rowley et al., 1995; Patzkowsky et al., 1999). Models of zonal circulation over Pangea require the migration of warm, moist air masses from the Tethys Ocean westward across Pangea, whereas models of monsoonal circulation diverted equatorial air masses from the Tethys Ocean to the midlatitude regions of the summer hemisphere (Fig. 1), leaving the Pangean equatorial latitudes relatively arid. Neither of these hypothesized circulation patterns sufficiently explains the anomalously heavy $\delta^{18}O$ values of pedogenic minerals in Permian paleosols from north-central Texas. As air masses move across a continent from a marine source they progressively "rain out" heavier isotopes, leaving more depleted $\delta^{18}O$ precipitation in the interiors and lee sides of continents (Dansgaard, 1964; Rozanski et al., 1993). This pattern is especially enhanced when air masses migrate over highlands or plateaus, such as the Himalayan-scale Alleghenian–Hercynian mountains that spanned equatorial Pangea during Late Pennsylvanian through Early Permian time (Fig. 1; Rowley et al., 1985; Crowley and Baum, 1992; Crowley et al., 1993; Crowley, 1994; Parrish, 1993, 1995; Ziegler et al., 1996). Thus, the $\delta^{18}O$ compositions of Permian pedogenic phyllosilicates and calcites from the Permo-Pennsylvanian paleosols we studied suggest that soil waters, and by inference meteoric waters, were likely derived from more local sources, such as the Midland and Delaware basin located directly west of the study area.

## 5. SUMMARY

Mineralogical and chemical compositions of pedogenic calcite and the fine ($<2$ and $<0.2$ $\mu$m) size phyllosilicate fractions

of Upper Pennsylvanian and Lower Permian paleosols from north-central Texas define down-profile trends typical of modern weathering profiles, indicating that pedogenic clays dominate the phyllosilicate fractions in these paleosols. Although there is evidence for a minor detrital component in the $<0.2$-$\mu$m phyllosilicate fraction, the $\delta^{18}O$ values of phyllosilicates and contemporaneous pedogenic carbonates from these paleosols exhibit a long-term enrichment that is consistent with a shift from more humid conditions during Late Pennsylvanian time to more arid conditions during Permian time. Estimated $\delta^{18}O$ compositions of Late Pennsylvanian and Early Permian precipitation for this region is inconsistent with previously hypothesized zonal or monsoonal atmospheric circulation over western equatorial Pangea. We interpret the $\delta^{18}O$ compositions of pedogenic minerals in the studied paleosols to record a local source of precipitation in this region, such as the Midland and Delaware Seas of the western coast of equatorial Pangea.

This study, in conjunction with previously published studies of the oxygen isotopic composition of pedogenic phyllosilicates, clearly demonstrates the potential of these minerals as proxies of paleoclimate and paleoenvironment. However, several aspects of the phyllosilicate fine fraction in paleosols, such as intermixture of different minerals, variable grain size that may represent different generations of crystal growth associated with isotopically distinct fluids, and variable chemical composition, presently limit their potential as paleoclimate proxies. These problems are minimized by analysis of "pure" mineralogical phases. Future studies should focus on isolation of pure mineralogical phases through separation techniques that use the distinctly different chemical and physical properties of phyllosilicate minerals, such as electrophoresis (Drever, 1969; Park and Lewis, 1969).

*Acknowledgments*—We are indebted to Bill DiMichele and Dan Chaney, Department of Paleobiology, Smithsonian Institution, for providing an introduction to the study area and a stratigraphic and paleoecologic framework. We also thank the Soil Science graduate pedology class at the University of California–Davis for allowing us to use XRD data collected from modern soils. D. G. McGahan provided graphical expertise. This research received support from an NSF IGERT "Nanomaterials in the Environment, Agriculture, and Technology," in addition to Grants-in-Aid to N. Tabor from the Geological Society of America, the American Association of Petroleum Geologists, the Society for Sedimentary Geology (SEPM), and Sigma Xi, as well as NSF grant EAR-9814640 to I. P. Montanez. We thank Martin Goldhaber and two anonymous reviewers for constructive reviews that considerably improved the manuscript.

*Associate editor:* M. B. Goldhaber

## REFERENCES

Allen B. L. and Hajek B. F. (1989) Mineral occurrence in soil environments. In *Minerals in Soil Environments* (eds. J. B. Dixon and S. B. Weed), pp. 199–278. Soil Sci. Soc. Am..

Amundson R., Chadwick O. A., Kendall C., and Wang Y. (1996) Isotopic evidence for shifts in atmospheric circulation patterns during the Late Quaternary in mid–North America. *Geology* **24,** 23–26.

Anderson J. U. (1963) An improved pretreatment for mineralogical analysis of samples containing organic matter. *New Mexico St. Univ. Agr. Exper. Sta.* **172,** 380–388.

April R. H., Hluchy M. M., and Newton R. M. (1986) The nature of vermiculite in Adirondack soils and till. *Clays Clay Miner.* **34,** 549–556.

Bain D. C., Mellor A., and Wilson M. J. (1990) Nature and origin of an aluminous vermiculitic weathering products in acid soils from upland catchments in Scotland. *Clay Min.* **25,** 467–475.

Barron E. J. and Moore G. T. (1994) Climate Model Application in Paleoenvironmental Analysis. *Soc. Sed. Geol. Short Course* **33**.

Barron E. J. and Fawcett P. J. (1995) The climate of Pangaea: A review of climate model simulations of the Permian. *The Permian,* Vol. 1 (eds. P. Scholle, T. Peryt, and D. S. Umer-Scholle(eds.; Springer-Verlag.

Bird M. I. and Chivas A. R. (1988) Stable-isotope evidence for low-temperature kaolinitic weathering and post-formational hydrogen-isotope exchange in Permian kaolinites. *Chem. Geol.* **72,** 249–265.

Bird M. I. and Chivas A. R. (1989) Stable isotope geochronology of the Australian regolith. *Geochim. Cosmochim. Acta* **53,** 3239–3256.

Brown R. W. (1977) A sample fusion technique for whole rock analysis with the electron microprobe. *Geochim Cosmochim Acta* **41,** 435–438.

Brown Jr. L. F., Solis Irarte R. F., and Johns D. A. (1987) Regional stratigraphic cross sections, Upper Pennsylvanian and Lower Permian Strata (Virgillian and Wolfcampian Series), north-central Texas. *Bur. Econ. Geol.* **27** p.

Buol S. W., Hole F. D., McCracken R. J., and Southard R. J. (1997) *Soil Genesis and Classification.* Iowa State University Press.

Cerling T. E. (1984) The stable isotopic composition of modern soil carbonate and its relationship to climate. *Earth Planet. Sci. Lett.* **71,** 229–240.

Cerling T. E. and Quade J. (1993) Stable carbon and oxygen isotopes in soil carbonates. *Geophys. Monogr.* **78,** 217–231.

Chamley H. (1989) *Clay Sedimentology.* Springer-Verlag.

Clayton R. N. and Mayeda T. K. (1963) The use of bromine pentafluoride in the extraction of oxygen from oxides and silicates for isotopic analysis. *Geochim. Cosmochim. Acta* **27,** 43–52.

Craig H. (1957) Isotopic standards for carbona and oxygen and correction factors for mass-spectrometric analysis of carbon dioxide. *Geochim. Cosmochim. Acta* **12,** 133–149.

Crowley T. J. (1994) Pangean climates. *Pangea: Paleoclimate, Tectonics, and Sedimentation During Accretion, Zenith, and Breakup of a Supercontinent* (ed. G. D. Klein), pp. 25–40. Geological Society of America, Special Paper 288.

Crowley T. J. and Baum S. K. (1992) Modeling late Paleozoic glaciation. *Geology* **20,** 507–510.

Crowley T. J., Yip K. J., and Baum S. K. (1993) Milankovitch cycles and Carboniferous climate. *Geophys. Res. Lett.* **20,** 1175–1178.

Crawford-Elliot W., Savin S. M., Dong H., and Peacor D. R. (1997) A paleoclimate interpretation derived from pedogenic clay minerals from the Piedmont Province, Virginia. *Chem. Geol.* **142,** 201–211.

Dansgaard W. (1964) Stable isotope in precipitation. *Tellus* **16,** 436–468.

Deutz P., Montanez I. P., Monger H. C., and Morrison J. (2001) Morphology and isotope heterogeneity of Late Quaternary pedogenic carbonates: Implications for paleosol carbonates as paleoenvironmental proxies. *Palaeogeogr. Palaeoclim. Palaeoecol.* **166,** 293–317.

Drever J. I. (1969) The separation of clay minerals by continuous particle electrophoresis. *Am. Miner.* **54,** 937–942.

Elliot C. W., Savin S. M., Dong H., and Peacor D. R. (1997) A paleoclimate interpretation derived from pedogenic clay minerals from the Piedmont Province, Virginia. *Chem. Geol.* **142,** 201–211.

Faure G. (1986) *Principles of Isotope Geology.* Wiley.

Foscolos A. E. (1990) Catagenesis of argillaceous sedimentary rocks: Diagenesis. (eds. Mcilreath I. A., Morrow W.) pp. 177–188. Geoscience Canadian Reprint Series 4.

Francis J. E. (1993) Palaeoclimates of Pangea—Geological evidence. *Can. Soc. Petr. Geol. Mem.* **17,** 265–274.

Frye J. C., Glass H. D., and William H. B. (1968) Mineralzonation of Woodfordian loesses of Illinois. *Illinios St. Geol. Surv. Circ.* **427,** 44.

Gonfiantini R. (1978) Standards for stable isotope measurements in natural compounds. *Nature* **271,** 534–536.

Gonfiantini R. (1984) Advisory Group Meeting on Stable Isotope Reference Samples for Geochemical and Hydrological Investigations. *Rep. Dir. Gen. IAEA.*

Gregory R. R. (1991) Oxygen isotope history of seawater revisited: Timescales for boundary event changes in the oxygen isotope com-

position of seawater. In *Stable Isotope Geochemistry: A Tribute to Samuel Epstein.* (eds. Taylor H. P., O'Neil J. R., and Kaplan I. R.), pp. 65–76. Geochemical Society.

Hentz T. F. (1988) Lithostratigraphy and paleoenvironments of upper Paleozoic continental red beds, north-central Texas: Bowie (new) and Wichita (revised) groups: The University of Texas at Austin. *Bur. Econ. Geol. Rep. Invest.* **170**.

Hoefs J. (1997) *Stable Isotope Geochemistry*. Springer-Verlag.

Holland H. D. (1984) *The Chemical Evolution of the Atmosphere and Oceans. Princeton Series in Geochemistry*. Princeton University Press.

Hsieh J. C. C. (1996) *An isotopic study of soil water and pedogenic clays in Hawaii.* Ph.D. thesis. Cal. Instit. Tech.

Hsieh J. C. C., Chadwick O. A., Kelly E. F., and Savin S. M. (1998) Oxygen isotopic composition of soil water: Quantifying evapotranspiration and transpiration. *Geoderma* **82,** 269–293.

Hudson J. D. and Anderson T. F. (1989) Ocean temperatures and isotopic compositions through time. *Trans. R. Soc. Edinburgh Earth Sci.* **40,** 183–192.

Ismail G. T. (1969) Role of ferrous iron oxidation in the alteration of biotite and its effect on the type of clay minerals formed in soils of arid and humid regions. *Am. Mineral.* **54,** 1460–1466.

Jackson M. L. (1979) *Soil Chemical Analysis—Advanced Course*. Self-published by the author, Madison, Wisconsin.

Kim S. and O'Neil J. R. (1997) Equilibrium and nonequilibrium oxygen isotope effects in synthetic carbonates. *Geochim. Cosmochim. Acta* **61,** 3461–3475.

Lawrence J. R. and Taylor Jr. H. P. (1971) Deuterium and oxygen-18 correlation: Clay minerals and hydroxides in Quaternary soil compared to meteoric water. *Geochim. Cosmochim. Acta* **35,** 993–1003.

Lawrence J. R. and Taylor Jr. H. P. (1972) Hydrogen and oxygen isotope systematics in weathering profiles. *Geochim. Cosmochim. Acta* **36,** 1377–1393.

Lawrence J. R. and Rashkes Meaux J. R. (1993) The stable isotopic composition of ancient kaolinites of North America. *Geophys. Monogr.* **78,** 249–261.

Lecuyer C. and Allemand P. (1999) Modeling of the oxygen isotopic evolution of the seawater: Implications for the climate interpretation of the$\delta^{18}$O of marine sediments. *Geochim. Cosmochim. Acta* **63,** 351–361.

Lohmann K. C. and Walker J. C. G. (1989) The $^{18}$O record of Phanerozoic abiotic marine calcite cements. *Geophys. Res. Lett.* **16,** 319–322.

Mankin C. J. (1970) Introduction to the symposium papers on environmental aspects of clay minerals. *J. Sed. Petrol.* **40,** 788–854.

Moniz A. C., Buol S. W., and Weed S. B. (1982) Formation of an Oxisol-Ultisol transition in Sao Paulo, Brazil: II. Lateral dynamics of chemical weathering. *Soil Sci. Soc. Am. Proc.* **46,** 1234–1239.

Moore D. M. and Reynolds R. C. (1997) *X-ray Diffraction and the Identification and Analysis of Clay Minerals*. Oxford University Press.

Ojanuga A. G. (1973) Weathering of biotite in soils of a humid tropical climate. *Soil Sci. Soc. Am. Proc.* **37,** 644–646.

O'Neil J. R., Clayton R. N., and Mayeda T. K. (1969) Oxygen isotope fractionation in divalent metal carbonates. *J. Chem. Phys.* **51,** 5547–5558.

Park R. G. and Lewis G. C. (1969) Electrophoretic separation and fractionation of clay mixtures. *Am. Mineral.* **54,** 1473–1477.

Parrish J. T. (1993) Climate of the supercontinent Pangea. *J. Geol.* **101,** 215–233.

Parrish J. T. (1995) Geologic evidence of Permian climate. In *The Permian of Northern Pangean*, Vol. 1 (eds. P. A. Scholle, T. Peryt, and D. S. Umer-Scholle), pp. 53–61. Springer-Verlag.

Patzkowsky M. E., Smith L. H., Markwick P. J., Engberts C. J., and Gyllenhaal E. D. (1999) Application of the Fujita-Ziegler paleoclimate model: Early Permian and Late Cretaceous examples. *Palaeogeogr. Palaeoclim. Palaeoecol.* **86,** 67–85.

Pearson P. N., Ditchfield P. W., Singano J., Harrcourt-Brown K. G., Nicholas C. J., Olsson R. K., Shackleton N. J., and Hall M. A. (2001) Warm tropical sea surface temperatures in the Late Cretaceous and Eocene Epochs. *Nature* **413,** 481–487.

Quade J., Cerling T. E., and Bowman J. R. (1989) Systematic variations in the carbon and oxygen isotopic composition of pedogenic carbonate along elevation transects in the southern Great Basin. *Geol. Soc. Am. Bull.* **101,** 464–475.

Rasbury T. E., Hanson G. N., Meyers W. J., Holt W. E., Goldstein R. H., and Saller A. H. (1998) U-Pb dates of Paleosols: Constraints on late Paleozoic cycle durations and boundary ages. *Geology* **26,** 403–406.

Retallack G. J. (1988) Field recognition of paleosols. *Paleosols and Weathering through Geologic Time: Principles and Applications* (eds. J. Reinhardt and W. R. Sigleo), pp. 1–20. Geological Society of America, Special Paper 216.

Retallack G. J. (1994) A pedotype approach to latest Cretaceous and earliest Tertiary paleosols in eastern Montana. *Geol. Soc. Am. Bull.* **106,** 1377–1397.

Ross C. A., Baud A., and Menning M. (1994) A timescale for Project Pangea. *Mem. Can. Soc. Petrol. Geol.* **17,** 81–83.

Rowley D. B., Raymond A., Parrish J. T., Lottes A. L., Scotese C. R., and Ziegler A. M. (1985) Carboniferous paleogeographic, phytogeographic, and paleoclimatic reconstructions Inter. *J. Coal Geol.* **5,** 7–42.

Rozanski K., Araguas-Araguas L., and Gonfiantini R. (1993) Isotopic patterns in modern global precipitation. *Geophys. Monogr.* **178,** 1–36.

Ruppel S. C. and Hovorka S. D. (1995) Controls on reservoir development in Devonian chert: Permian basin, Texas. *Am. Assoc. Petrol. Geol. Bull.* **79,** 1757–1785.

Savin S. M. and Epstein S. (1970) The oxygen and hydrogen isotope geochemistry of clay minerals. *Geochim. Cosmochim. Acta* **34,** 25–42.

Savin S. M. and LeeM. (1988) Isotopic studies of phyllosilicates. In Hydrous Phyllosilicates (Exclusive of Micas). (ed. Bailey S. W.), *Reviews in Minerology*, **19**, pp. 189–223.

Savin S. M. and Hsieh J. C. C. (1998) The hydrogen and oxygen isotope geochemistry of pedogenic clay minerals: Principles and theoretical background. *Geoderma* **82,** 227–253.

Scotese C. R. (1984) Paleozoic paleomagnetism and the assembly of Pangea. In *Plate Reconstruction from Paleozoic Paleomagnetism, Geodynamics Series.* (eds. Van der Voo R. and Scotese C. R.), **12**, pp. 1–10.

Sheppard S. M. F. (1986) Characterization of isotopic variations in natural waters. In *Stable Isotopes in High Temperature Geological Processes.* (eds. Valley J. W., Taylor H. P., and O'Neil J. R.), *Reviews in Minerology* **16**, pp. 165–181.

Sheppard S. M. F. and Gilg H. A. (1996) Stable isotope geochemistry of clay minerals. *Clay Minerals* **31,** 1–24.

Singer A. (1980) The paleoclimate interpretation of clay minerals in soils and weathering profiles. *Earth-Sci. Rev.* **303,** 326.

Soil Survey Staff (1998) *Keys to Soil Taxonomy*. United States Department of Agriculture, Natural Resources Conservation Service.

Sparks D. L. (1995) *Environmental Soil Chemistry*. Academic Press.

Srodon J. (1999) Use of clay minerals in reconstructing geological processes: Recent advances and some perspectives . *Clay Minerals* **34,** 27–37.

Stern L. A., Page Chamberlain C., Reynolds R. C., and Johnson G. D. (1997) Oxygen isotope evidence of climate change from pedogenic clay minerals in the Himalayan molasse. *Geochim. Cosmochim. Acta* **61,** 731–744.

Taylor H. P. (1986) Igneous rocks: II. Isotopic case studies of circumpacific magmatism. In *Stable Isotopes in High Temperature Geological Processes.* (eds. Valley J. W., Taylor H. P., and O'Neil J. R.), *Reviews in Minerology* **16**, pp. 373–318.

Taylor H. P. and Sheppard S. M. F. (1986) Igneous rocks: I. Processes of isotopic fractionation and isotope systematics. In *Stable Isotopes in High Temperature Geological Processes.* (eds. Valley J. W., Taylor H. P., and O'Neil J. R.), *Reviews in Minerology* **16**, pp. 227–269.

Van der Voo R., Peinado J., and Scotese C. R. (1984) A paleomagnetic reevaluation of Pangea reconstructions. In *Plate Reconstruction from Paleozoic Paleomagnetism, Geodynamics Series.* (eds. Van der Voo R. and Scotese C. R.), *Geodynamics Series* **12**, pp. 11–27.

Vicente M. A., Razzaghe M., and Robert M. (1977) Formation of aluminium hydroxy vermiculite (intergrade) and smecite from mica under acidic conditions. *Clay Minerals* **12,** 101.

Veizer J. (1999) $^{87}Sr/^{86}Sr$,$\delta^{13}C$, and$\delta^{18}O$ evolution of Phanerozoic seawater. *Chem. Geol.* **161,** 59–88.

Wilson M. J. (1993) Pedologic factors influencing the distribution and properties of siol smectites. *Trends Agric. Sci.* **1,** 199–216.

Wilson M. J. (1999) The origin and formation of clay minerals in soils: Past, present and future perspectives. *Clay Minerals* **34,** 7–25.

Yemane K., Kahr G., and Kelts K. (1996) Imprints of post-glacial climates and palaeogeography in the detrital clay mineral assemblages of an Upper Permian fluviolacustrine Gondwana deposit from northern Malawi. *Palaeogeogr. Palaeoclim. Palaeoecol.* **125,** 27–49.

Yapp C. J. (1990) Oxygen isotopes in Fe(III) oxides, 2: Possible constraints on the depositional environment of a Precambrian quartz–hematite banded information. *Chem. Geol.* **85,** 337–344.

Yapp C. J. (1993) The stable isotope geochemistry of low temperature Fe(III) and Al“oxides” with implications for continental paleoclimates. *Geophys. Monogr.* **78,** 285–294.

Ziegler A. M., Hulver M. L., and Rowley D. B. (1996) Permianworld topography and climate. In *Late Glacial and Postglacial Environmental Changes—Quaternary, Carboniferous–Permian and Proterozoic* (ed. I. P. Martini(ed.; Oxford University Press.